

A Multi-Agent Security Testbed for the Analysis of Attacks and Defenses in Collaborative Sensor Fusion

R. Spencer Hallyburton
Duke University
spencer.hallyburton@duke.edu

David Hunt
Duke University
david.hunt@duke.edu

Shaocheng Luo
Duke University
shaocheng.luo@duke.edu

Miroslav Pajic
Duke University
miroslav.pajic@duke.edu

Abstract—The performance and safety of autonomous vehicles (AVs) deteriorates under adverse environments and adversarial actors. The investment in multi-sensor, multi-agent (MS/MA) AVs is meant to promote improved efficiency of travel and mitigate safety risks. Unfortunately, minimal investment has been made to develop security-aware MS/MA sensor fusion pipelines leaving them vulnerable to adversaries. To advance security analysis of AVs, we develop the Multi-Agent Security Testbed, MAST, in the Robot Operating System (ROS2). Our framework is scalable for general AV scenarios and is integrated with recent multi-agent datasets. We construct the first bridge between AVstack and ROS and develop automated AV pipeline builds to enable rapid AV prototyping. We tackle the challenge of deploying variable numbers of agent/adversary nodes at launch-time with dynamic topic remapping. Using this testbed, we motivate the need for security-aware AV architectures by exposing the vulnerability of centralized multi-agent fusion pipelines to (un)coordinated adversary models in case studies and Monte Carlo analysis.

I. INTRODUCTION

Adversarial actors, sensor degradation due to adverse environments, and unavoidable natural occlusion threaten the prospect of safely deploying autonomous vehicles (AVs) in the real world. AVs that are ill-equipped for these challenging conditions are at risk for devastating safety-critical failures. The severity of such outcomes is apparent with recent real-world case studies: white-hat adversaries exposed that hackers could gain remote access to a vehicle’s control center and manipulate messages on the CAN bus [27]; a “state-of-the-art” commercially-available AV endured a high-speed collision due simply to sun reflecting off of a large vehicle and obscuring perception [11]; natural occlusions were shown to cause delayed brake response time due to deteriorated motion prediction accuracy [25]. Moreover, a recent report from the National Highway Traffic Safety Administration (NHTSA) described the increasing concerns in adversarial remote exploitation of vehicle hardware and software and illuminated the lack of security protocols that could mitigate threats [28].

Challenging environments and adversarial actors are formidable barriers for a single agent to overcome. An important avenue for mitigating adversity is to pursue multi-sensor, multi-agent (MS/MA) collaborative autonomy. Multi-sensor systems leverage multiple sensing modalities including but not limited to cameras, LiDARs, and radars. Multi-agent

systems share information with external platforms via vehicle-to-vehicle (V2V) and vehicle-to-infrastructure (V2I) channels. Such MS/MA concepts are essential to the security awareness of perception, planning, and control because they provide complementary perspectives and add necessary redundancy over single-source sensors.

Government and industry have been investing heavily in MS/MA vehicle technology for over a decade. Experts have used this investment to foreshadow high operating ranges [1], low latency [6], and robust physical testing infrastructure for academic research [4], [5]. The investment in connected vehicle technologies is meant to improve travel efficiency and mitigate immediate safety risks. Unfortunately, it coincides with a dramatic rise in cyber threats against cyber-physical systems (CPS) [35]. In particular, the confluence of demonstrated remote attacks on AVs with the desire to expand networked connectivity of AVs suggest an impending increase in cyber threats against AVs that could compromise MS/MA pipelines.

Despite the investment in connected vehicles, *minimal effort has been made to develop security-aware MS/MA collaborative algorithms*. To spark development in this critical area, we design and implement a scalable **multi-agent security testbed, MAST**, based on v2 of the Robot Operating System (ROS2 [30]). With MAST, an evaluator can spin up multiple mobile and static (infrastructure) agents and evaluate MS/MA pipelines under benign and adverse conditions including security threats. MAST is released open-source¹.

MAST uses open-source datasets to feed MS/MA sensor data to agent nodes in an event-driven simulation. The recently-released MS/MA dataset generation pipeline from [17] provides a general framework to generate limitless MS/MA data from complex scenes with multiple mobile and static agents. We integrate the datasets from [17] and illustrate their effectiveness in exploring multi-agent security case studies.

MAST also uses the advanced control algorithms and perception models developed for AVs in a real-time manner, which are provided by AVstack [19], an emerging platform for the design, implementation, testing, and analysis of AVs. However, prior to this work, AVstack was only used in an offline, postprocessing context. To integrate AVstack with the near-real-time environment of MAST, we leverage the real-time capabilities of ROS and develop the first bridge between AVstack and ROS. This bridge is released open-source².

In MAST, we bridge the gap between AV pipelines and the module menagerie implemented in AVstack by developing automated pipeline builds. The build process uses *registries*

¹redacted

²redacted

inspired by OpenMMLab [15]. Prior to execution, the designer will specify the configuration of the AV pipeline in a high-level language in MAST. At launch-time, the build process will build each module of the AV pipeline by searching for algorithms in the registries. This process simplifies executing case studies and Monte Carlo analysis and yields faster deployment.

To advance security analysis of MS/MA autonomy in MAST, we implement baseline adversary nodes capable of disrupting sensing, perception, or tracking operations in the AV pipeline. We consider both uncoordinated and coordinated models of multi-adversary attacks on multi-agent systems. In the former, decisions of each adversary are independent. In the latter, adversaries can collude to consistently compromise multiple agents. To consider realistic scenarios, we consider that only a subset of agent nodes are compromised by adversaries. To handle a variable number of agents and adversaries at launch-time, we create a dynamic topic remapping approach that allows us to insert a number of adversaries into the agent pipelines without modifying downstream algorithms/nodes.

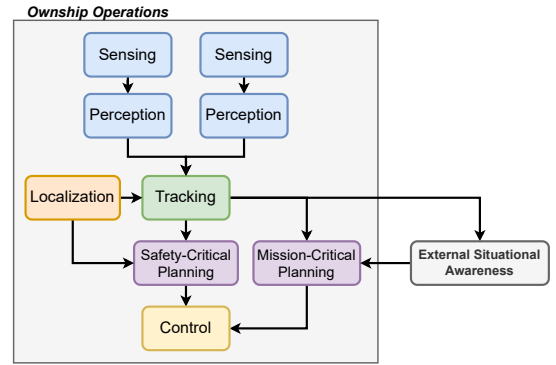
As an evaluation, we provide case studies with multiple adversary models on multi-agent datasets to illustrate the effectiveness of MAST in performing security analysis. We explore how (un)coordinated adversaries can affect multi-agent sensor fusion through in-depth case studies with visualizations of sensory, perceptive, and tracking data for each agent. Videos of case studies are released online³. Finally, we demonstrate running a Monte Carlo analysis by scripting over MAST to capture high-level insights into the robustness of existing fusion pipelines to adversarial actors. We find that the lack of security awareness in vanilla sensor fusion pipelines leaves collaborative autonomy dangerously vulnerable to exploitation.

In summary, this work makes the following contributions:

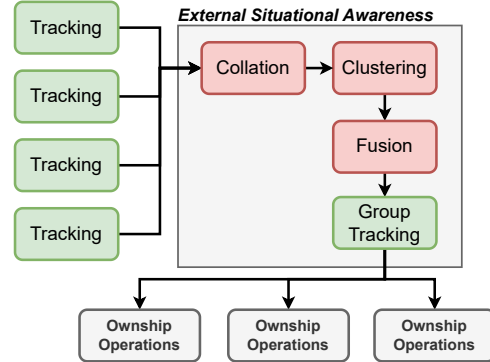
- We design MAST, the multi-agent security testbed, using ROS2 for security-analysis of MS/MA autonomy.
- We integrate MAST with the recently-released multi-agent dataset pipeline [17] for the first real-time playback of simulated MS/MA autonomy data.
- We build the first bridge between AVstack [19] and ROS to integrate state-of-the-art AV algorithms into a scalable, near-real-time simulation.
- We design an automated build process for AV algorithm pipelines using high-level configuration files to enable rapid prototyping of MS/MA configurations.
- We provide a baseline framework for security analysis of MS/MA algorithms in MAST with (un)coordinated models of adversary nodes that can affect the sensing, perception, tracking, and/or communication of AVs.
- We execute security-focused case studies and Monte Carlo evaluations with centralized sensor fusion and motivate the need for security-aware collaborative autonomy.

II. MULTI-AGENT COLLABORATION

Due to the *safety-critical* nature of AVs and the vulnerabilities induced by opening wireless communication channels, safety-critical features such as adaptive cruise control, lane centering, and obstacle avoidance will be influenced primarily by local information. Multi-agent collaboration will play a significant role in the validation of local information and in



(a) Ownship operations for each agent fusing external awareness for mission-critical planning.



(b) Centralized fusion via command center to provide unified operating picture across multiple agents.

Fig. 1: (a) Ownship operations use local information for safety-critical planning and incorporate external knowledge for mission-critical. Safety-critical is partitioned to mitigate impact of adversarial actors in the sensing network. (b) Command center integrates situational awareness from all agents. Collation synchronizes data while clustering, fusion, and group tracking distill agents’ tracks into a unified operating picture.

mission-critical functions such as broad situational awareness, path-planning, and urban maneuvering.

Both on-board and collaborative computation will occur. We choose to partition each agent’s sensor fusion pipeline into two estimators: (1) safety-critical estimator that depends only on ownship information to ensure the safety and security of essential tasks, and (2) a mission-critical estimator that incorporates information from both local and collaborative/distributed systems. Fig. 1 demarcates the roles of onboard and distributed computation in a multi-agent system. Information is passed between the local and external systems via wired/wireless communication channels. We consider centralized collaboration where a “command center” (CC) operates as an edge server that fuses information from multiple agents.

A. Safety-Critical Sensor Fusion

AV operations such as localization, lane centering, adaptive cruise control, and obstacle avoidance are safety-critical functions for the AV. To mitigate the impact of an adversary at the communication channels or in the unknown network of “collaborative” systems, these functions may rely only on local information. In this model, each agent assumes he is not compromised and that local information is sufficient to maintain safety-critical levels of performance.

³<https://sites.google.com/view/cpsl-mast/home>

B. Mission-Critical Sensor Fusion

Many of the functions in an AV are mission-critical. Failure of a module will impact the quality of service in the form of traffic delays, erroneous/compromised data reconnaissance, improper routing, erratic behavior, or an inability to move due to a forced system shutdown. Modules including high-level route optimization and medium-scale path planning via an awareness of nearby object states are considered mission critical and can benefit from collaborative sensor fusion.

C. Implementation Details

Here we present the implementation details of the agent and CC algorithms. For simplicity, we fix these pipelines throughout the case studies and Monte Carlo evaluations of Section VI. As illustrated in Section III-E, rearchitecting agent and CC algorithm pipelines is a simple process with `config`-based builds and will be included in future works. We consider a scenario where agents are estimating states of objects (e.g., other vehicles) in the environment and the CC is fusing object states gathered from the agents.

1) Dataset

The case studies and results in this work use the CARLA infrastructure dataset [17]. The dataset consists of one mobile agent (“ego”) and many static agents (“infrastructure”). The ego is connected to the ground plane via the vehicle chassis. The infrastructure agents are placed at dedicated positions in the scene to emulate a smart-city configuration. The infrastructure agents reside at 15 m elevations with a 30° downward pitch for an advantageous vantage point.

2) Agent Pipelines

Each agent has its own pipeline to filter and process ownership sensing data. The agent then sends estimated object states to the CC to be collated and fused. This model of sending high-level tracked states is consistent with the bandwidth and latency requirements of existing and future V2X systems [1].

a) Sensing. Each agent is equipped with a 10 Hz forward-facing RGB camera with a 90° field of view, a 1.4 fstop, and a 5 ms shutter. These parameters can be modified during dataset generation [17]. Each agent also possesses a rotating 64-channel LiDAR sensor time-synchronized with its camera. The ego’s LiDAR has an elevation span of $[-17.6^\circ, 2.4^\circ]$ (0° is straight forward) with full azimuth coverage. The infrastructure LiDAR spans $[-25^\circ, 30^\circ]$ with 90° azimuth coverage to provide a hybrid forward/bird’s-eye-view.

b) Perception. Sensor data are stored in datasets meaning the agents paths cannot be altered during MAST evaluation. To take advantage of this “replay” context for efficiency, we apply perception to LiDAR data offline and generate detections prior to running MAST. We use models provided by OpenMMLab [15] via `AVstack` [19]. During the evaluations, we replay the detections in lieu of raw sensor data since the agent dynamics are fixed.

c) Tracking. Detections are instantaneous estimates of object state. This state typically consists of positioning and sizing information. To build a longitudinal estimate of object state, detections are passed to multi-object tracking algorithms that score for object existence probabilities and associate incoming detections with existing tracked objects. Longitudinal

states are necessary for prediction and planning. We use multi-object tracking algorithms provided by [19]. These are classical algorithms using bipartite matching (e.g., [21]) for assignment and extended Kalman filtering for state estimation (e.g., [9]).

3) Command Center Pipeline

The advent of V2X communication and the investment in smart-city networking technologies will enable computation at edge server nodes [2]. We model that mobile and static agents are connected via wireless/wired interfaces, respectively. This configuration is motivated by the University of Michigan’s MCity [2]. In this configuration, infrastructure agents send estimated object states to the CC over wired connections while mobile agents experience higher latency and lower bandwidth over wireless (e.g., C-V2X or 802.11p transceivers [1]–[3]).

a) Collation. In a complex network of agents, messages will arrive asynchronously. While MAST can replay data either synchronously or asynchronously, perfect synchronicity is infeasible in the real world. To handle the practical case of asynchronous transmission, the CC maintains a circular, min-heap priority queue for each agent in the network to collate the data. At a predefined and tunable latency factor, the collation algorithm will determine the earliest viable timestamp and pop a batch of track states closest to that time from each of the agents. Each of the tracks is transformed such that all tracks are in a common frame of reference (e.g., “world” frame).

b) Clustering. Agents with overlapping fields of view may each obtain a track on the same physical object. However, the agents will not intrinsically know these tracks follow the same object. To merge common track states across the multiple agents, the CC clusters tracks from different agents using the tracks’ position states. The clustering algorithm is provided by `AVstack` [19] and is a simplified case of the classical DBSCAN algorithm. The output is a set of track clusters that each aspire to represent a single, unique object in the scene.

c) Fusion. Depending on the agents’ field of view overlap, the clusters may have one or more members where each member is from a different agent. The state estimates from each of the members are combined in the *fusion* step to distill a fused state estimate for each cluster. Since each member is a track and tracks have temporal correlations, we fuse member states using track-to-track fusion with the covariance intersection algorithm [22]. After fusion, each cluster has a representative state in addition to its track members.

d) Group Tracking. Clustering/fusion does not consider the temporal consistency of clusters. Thus, clusters lack longitudinally-consistent labels and existence probability scores. We use group tracking at the CC to pass fused estimates of cluster states as detections to tracking algorithms. This approach is a special case of the widely-studied field of *group tracking* that has extensive theory and algorithms [9]. The output of tracking is the CC’s estimate of the state of unique objects in the scene. These tracks are then fed back to each of the agents as mission-critical situational awareness.

III. MULTI-AGENT SECURITY TESTBED (MAST)

MAST is built on ROS2 to leverage the strong community of open-source robotics. We design MAST to be scalable for pursuing many-agent, many-sensor evaluations with both distributed and centralized fusion architectures. Here, we describe

the data sources, ROS nodes, and algorithm pipelines used to spin up MS/MA evaluations in MAST.

A. Multi-Agent Data Sources

Datasets from the recently-released multi-agent dataset generation framework [17] drive event-based simulations in MAST. The multi-agent datasets contain multi-modal perception data and ground truth object state information from static and mobile agents. In an event-based simulation, the playback rate can scale to support the required computation from each of the nodes; MAST can run faster or slower than the wall-clock time depending on the computation needs. In this way, MAST is not limited to a maximum number of agents/sensors.

B. ROS Nodes

The “node” is the base execution process in ROS. Nodes communicate messages across topics. Here, we describe the relevant nodes used to build MAST environments.

a) Simulator The simulator node drives the event loops. Agent pose and sensor data are read from the CARLA multi-agent dataset [17] and published at the desired rate. Ground-truth object information is also published.

b) Mobile Agent The CARLA dataset captures data from mobile agents spawned in the town. To simplify the experiments, we consider an infrastructure-only case where there is a single mobile agent (the “ego”).

c) Static Agents Infrastructure sensing is an important pillar of the future of multi-platform collaborative sensing. We spawn nodes for multiple infrastructure sensors nearby to the ego vehicle for V2X collaboration.

d) Command Center The CC is composed of broker and primary nodes. The broker polls to collect data from each of the agents and performs collation as described in Section II-C3. The broker sends collated data to the primary node; the primary node executes the remainder of the CC pipeline.

e) Adversary We model the network as if each agent were susceptible to an adversary. Uncoordinated adversaries attach to the compromised agent nodes directly. Coordinated adversaries live in the communication network and communicate with a special coordinator node that is responsible for synchronizing attack directives among adversaries.

f) Visualizer A QT-based visualizer runs to update the operator on the performance in real-time; an example frame is shown in Fig. 2. The visualizer subscribes to information furnished by the agents and is a useful debugging tool.

C. Launch-Time Flexibility and Scalability

Many multi-agent/security evaluations are tailored to a particular dataset or agent configuration. For example [34] generates an adversarial dataset, Adv-OPV2V [33], with adversary optimization prior to execution. Similarly, [14] develops a ROS framework for evaluating surface vessels but restricts operation to a single ego agent and a fixed number of agents a-priori. In contrast, MAST is scalable to an arbitrary number of agents and adversaries. Moreover, MAST is flexible enough to handle distributed and centralized sensor fusion and to handle a diversity of agent and CC algorithm pipelines. The scalability and flexibility of MAST were achieved via the following innovations to the ROS launch configuration files.

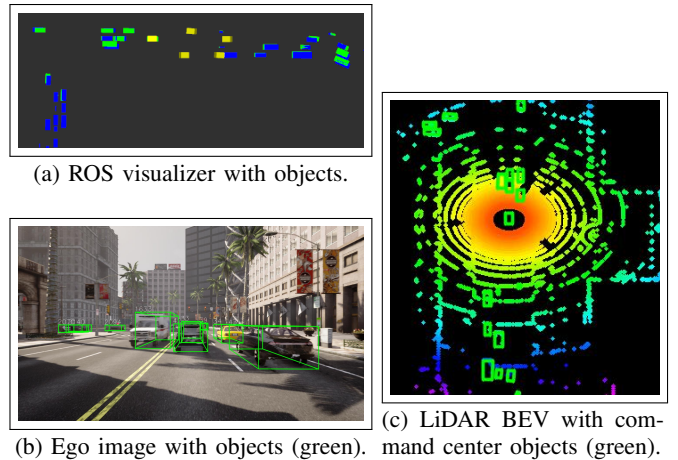


Fig. 2: (a) Bird’s-eye-view of multi-agent simulation under an unattacked scenario. Tracked object state estimates (green) overlap with ground truth object locations (blue). Agents (yellow) are positioned in the scene for case-study purposes and clearly do not provide full coverage over the town. Four infrastructure agents and one mobile agent (“ego”) provide object estimates to the CC. All tracks are pushed to the visualizer for real-time feedback. (b, c) Image and LiDAR data, respectively, from ego agent with tracked objects from command center overlaid in green.

a) Programmatic Node Launches A requirement for a flexible multi-agent evaluation framework is to specify the number of agent nodes at launch-time rather than hard-code the agents at build-time. We leverage recent advancements in ROS2 to design flexible launch files in a ‘bringup’ package. The launch files use `OpaqueFunctions` to defer scenario configurations to launch-time rather than the standard process of setting at built-time. This allows users to dynamically set the number of agent and adversary nodes.

b) Data Structures and Discovery Functions Multi-agent networks will experience range limitation, quality of service (QoS) variability, and packet drops. Unfortunately, many research works set a fixed number of agents for each run and assure via software that each agent communicates with zero latency and no drops. Many of the algorithms developed in these overly clean environments are ill-suited to handle the variability experienced in the real-world, i.e., they break in response to natural variability. To improve robustness of multi-agent evaluations, all data containers are circular, min-heap priorities queues to handle out-of-order or lost data. Moreover, the CC broker runs a discovery function that receives agent status messages. This allows the network to expand and contract without breaking data structures and algorithms.

c) Dynamic Topic Remapping In a general multi-agent analysis or a specific security analysis, it can be desirable to apply a function to a *subset* of the agent nodes (e.g., an adversary attacks sensor data of a single agent). To intercept inputs/outputs of an agent node and apply functions for any reason, we develop a dynamic ROS topic remapping solution for MAST. The launch file will dynamically remap the topic to pass through any specified intermediate functions before that topic is published for all subscribers. The downstream subscribers/nodes will not observe any accounting differences

when topics are remapped through intermediaries. This feature was essential in developing a scalable and reconfigurable multi-adversary, multi-agent framework.

D. Bridge to AVstack

AVstack unifies and streamlines the AV design and prototype process [19]. Unfortunately, it was previously limited to non-real-time applications because of the Python global interpreter lock (GIL). This meant that AVstack was only useful as a postprocessing and analysis tool. To support development of near-real-time AVs and to enable more flexible evaluations, we develop the first bridge between ROS and AVstack. AVstack provides libraries of tested algorithms from the open-source community for AV design while ROS defines a framework for scalable multiprocessing and communication; the bridge enables automatic conversion of datatypes and messages between the two. The bridge has been released open-source⁴ to support future AV development and evaluation.

E. Algorithm Pipelining and Configuration

MAST makes use of flexible python-based configuration files for automated building of sensor fusion pipelines. We take inspiration from OpenMMLab’s configuration management [15] and add algorithm registries to MAST and AVstack. Perception, tracking, clustering, and fusion algorithms are then configured in a high-level language such as in Configuration 1. Agents can run the same or different pipelines to suit the needs of the evaluation.

Configuration 1: Pipelines configured with simple python code.

```
# command_center_pipeline.py
commandcenter = dict(
    type="CommandCenter",
    pipeline = dict(
        type="CommandCenterPipeline",
        clustering=dict(
            type="SampledAssignmentClusterer",
            assign_radius=2.0),
        group_tracking=dict(
            type="GroupTrackerWrapper",
            fusion=dict(
                type="CovarianceIntersectionFusion"),
            tracker=dict(type="KalmanBoxTracker3D")
        )
    ))
```

IV. THREAT MODEL FOR SECURITY ANALYSIS

We present and evaluate two threat models in this work: (1) a subset of agents are independently compromised at the sensing or perception level in an “uncoordinated attack”, and (2) a subset of agents are compromised at the tracking or communication level by colluding adversaries in a “coordinated attack”. The diagram in Fig. 3 illustrates graphically the positioning of the adversary in each case.

Uncoordinated Attack Many existing security analyses focus on attacks at the sensing or perception level. One surface for this class of attack is to obtain physical access to the vehicle’s electronic components. Physical access was used in recent CPS security case studies [10], [13], [20], [23], [24]. Another attack surface is to infiltrate the physical

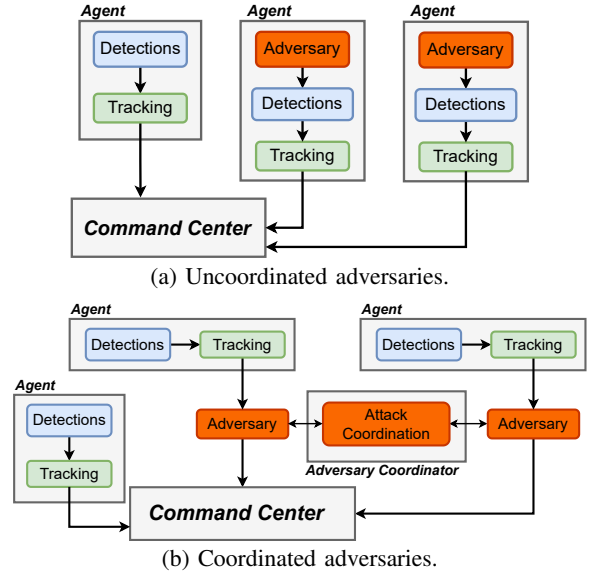


Fig. 3: (a) We model uncoordinated adversaries as directly manipulating detections from perception. Each adversary has its own local objective. This model can encompass physical access, sensing channels, and compromised model attack surfaces. (b) In the coordinated case, adversaries communicate with an attack coordinator to synchronize attack objective functions. We model this threat at the network level where communication links are compromised.

sensing channels via black-box [31] or white-box spoofing attacks [12] or physical adversaries objects [7], [32]. These attacks are “uncoordinated” - i.e., an adversary compromises sensing/detections of an AV without an ability to manipulate other AVs or communicate with other attacker nodes.

In an uncoordinated attack, each adversary is operating under its own malicious objective function. While the goal of the attackers may align (e.g., add fake objects), the implementation may be inconsistent across attackers (e.g., the location and/or type of attacks may differ).

We choose to model uncoordinated attacks as the attacker directly adding/removing detections at the output of perception. This model can account for physical access, sensing channels, and compromised perception attack surfaces.

Coordinated Attack Communication networks are needed in multi-agent contexts to distribute information among agents. Connecting potentially untrusted agents, infrastructure sensing, and edge servers presents a new class of threat models for AVs: *coordinated attacks*. Adversaries positioned in the communication network can leverage the network itself to synchronize attacks. Coordinated attacks are most likely to occur at the networking-level of a distributed system and can be realized as compromised Wi-Fi hotspots [26] or access points [8], [29].

A coordinated attack has all adversaries operating under a common objective function with pooled knowledge. The adversaries thus have their own “command-center” to coordinate the actions between them. For this reason, coordinated attacks are more powerful than uncoordinated attacks.

We choose to model coordinated attacks with the presence of an attack coordinator node. Adversaries send agent pose and tracked objects to the coordinator. It is the coordinator’s job to

⁴redacted

Parameter	Type
Num. of compromised agents	Int. on [0, # agents]
Pct. of existing detections manipulated	Pct on [0, 1.0]
Num. of false detections added	Positive integer
(Un)Coordinated	Boolean

TABLE I: Security analysis varies adversary capability including number of compromised nodes and level of data corruption.

decide on the false positive/negative targets and to share this information with each of the adversaries. The adversaries then apply this attack directive to their compromised agent.

A. Attack Knowledge and Capability

Uncoordinated attacks. We assume an adversary that has compromised an agent has full knowledge of the agent’s pose and perception data. We model the attacker as being able to directly modify the detections. This encapsulates the effects of manipulating physical channels (e.g., spoofing [16], [31], adversarial objects [7], [32]) or cyber-based attackers [18].

Coordinated attacks. A coordinated attack exists at the network level. As a result, attackers have access to both the agent’s pose and the agent’s estimated state of objects in the scene. These estimated states are in the form of object tracks with at least position, bounding-box, velocity, and orientation states. An attacker manipulates the estimated states of surrounding objects by adding false positives, removing tracks to create false negatives, or perturbing the state of an existing track to create a translation, as defined in [16].

B. Attacker Goals

The goal of the attackers in both threat models is to corrupt the situational awareness of the CC. This goal is impactful because of the redistribution of information to nearby agents; information flows from the CC back to all agents *including those agents who were not directly compromised by an adversary*, as described in Fig. 1. Distributing compromised information to agents interferes with mission-critical functions. We consider two objective attack goals in this work: the attacker wishes to (1) add fake (spoofed) objects (false positives), and (2) remove existing objects (false negatives) at the CC.

C. Attack Designs

The attack’s power is a function of the number of agents that are compromised and of the number of manipulations performed (i.e., number of false positives added, true objects negated). A more powerful attack has more compromised agents and/or performs more manipulations. Table I describes the design parameters evaluated in these security studies.

D. Attack Effectiveness

We evaluate attack effectiveness along two dimensions: (1) The attacker must remain stealthy to integrity algorithms from the CC. (2) The attacker is effective if he causes fake objects at the CC or if true objects in an agent’s field of view are not detected at the CC. To quantify attack success, we derive metrics to describe the agent/CC situational awareness compared to ground truth object locations.

We only attack the infrastructure sensors in this work and assume that situational awareness local to the ego vehicle is free from adversarial manipulation. This choice was made to focus our security analysis. An increased emphasis on

securing autonomous vehicles and the high degree of difficulty in exercising physical attacks on mobile AVs suggests that ownership information could be secured. Errors including false positives, false negatives, and noisy readings can still occur.

V. ATTACK EXECUTIONS

We present the attack executions. The attacker’s goal is to compromise the situational awareness at the CC while remaining stealthy to integrity algorithms. Attackers begin by selecting targets. Once targets are selected, the adversaries will manipulate data to achieve their target outcomes.

A. Target Object Selection

The two threat models differ in how they select false positive and false negative targets. The uncoordinated attack selects targets based purely on local information while in the coordinated attack, an adversary coordinator directs the targets.

Uncoordinated Attacks To select targets, each adversary uses the compromised agent’s detected objects as input to its own instance of the selection algorithm. Target false negatives are selected as some fraction of objects from an initial set of the agent’s detections. False positives are chosen as pseudo-random states within a maximum distance from the agent.

Coordinated Attacks Target selection occurs at the adversary coordinator. Each adversary sends uncompromised tracks from their host agent to the coordinator. The coordinator aligns the time and frame of all tracks and follows the selection algorithm of choosing target false negatives from clusters of objects and false positives as pseudo-random states close to any existing agent. After target selection, the coordinator sends the targets back to the adversaries who apply the directive.

B. Data Manipulation

The general framework of instantiating the attacks is identical in both the uncoordinated and coordinated cases given a selection of targets. After target selection, the adversary determines which detections/tracks to negate by performing an assignment between the agent’s detections/tracks and the target false negatives. Detections/tracks matching a false negative target are removed. False positive targets are propagated to the current time and appended to the detection/track list if they are within a maximum distance from the agent.

VI. EVALUATION

MAST is a useful tool for case studies and Monte Carlo evaluations. We present case studies and visualizations from (un)coordinated attacks against multi-agent collaborative fusion. We then present a Monte Carlo analysis over scenes and adversary configurations. In all cases, we fix the agent and CC pipelines as described in Section II for the simplicity of comparison. Fixing pipelines is not a requirement as MAST can easily spin up different pipelines using high-level configuration files. Table II provides the color map key for visualizations.

A. Case Studies

All case studies use scene #1 from the CARLA multi-agent dataset [17]. Four infrastructure sensors capture camera and LiDAR data from elevated positions near the ego vehicle.

The target selection of the uncoordinated adversaries and of the adversary coordinator follow the same *general* framework.

Box Color	Indication
White	The ground-truth state of an object with significant overlap with a detection/track. Always pairs with blue. “True positive”.
Blue	The detection/track state of an object with significant overlap with a ground-truth state. Always pairs with white. “True positive”.
Yellow	The ground-truth state of an object lacking overlap with a detection/track. “False negative”.
Red	The detection/track state of an object lacking overlap with a ground-truth state. “False positive”.
Green	Object state (any of ground truth, detection, or track) when no attempt at assignment/evaluation is made. For visualization only.

TABLE II: Case study visualizations color key.

In both cases, the target selector samples a number of false positives via $k_{FP} \sim \text{Pois}(\lambda)$ and a number of false negatives via $k_{FN} \sim r \cdot |D|$ where λ is the Poisson distribution parameter, r is a percentage, and $|D|$ is the number of objects detected by the agent in the uncoordinated case and the number of clusters in the coordinated case. We fix $\lambda = 5$ and $r = 20\%$ for all case studies. Fixing the parameters to be identical for both threat models means that more manipulations will occur in the uncoordinated case because there are a number of target selections happening equal to the number of adversaries compared to a single target selection for the coordinated case.

1) Baseline

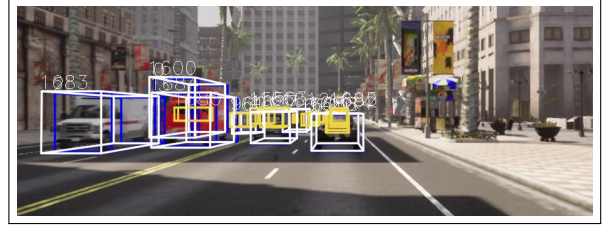
Natural occlusions between objects and limited sensor range will truncate the ego’s understanding of the environment. This will materialize as a number of false negatives from the ego’s local tracks, as seen in Figs. 4a, 4c. The centralized fusion of infrastructure sensing data can mitigate the incidence of false negatives by providing complementary perspectives. This benefit of multi-agent fusion is on display in Figs. 4b, 4d. Ego and infrastructure tracks are fused at the CC and redistributed to the ego for mission-critical planning. Multi-agent fusion has eliminated all false negatives from the ego’s situational awareness without introducing any false positives.

2) Uncoordinated Attack

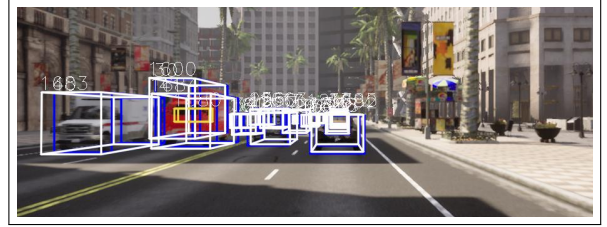
In an uncoordinated attack, adversaries select targets independent of each other. Following the threat model in Section IV, we simply model uncoordinated attacks as compromised detections at the output of perception.

Two adversaries latch on to two of the four infrastructure sensors. Each adversary compromises the agent locally without regard for the other. This creates false positives/negatives for the agents, as in Figs. 5a, 5c. The compromised agents send attacked state estimates to the CC. Without integrity to detect the attacks, the CC will be partially compromised. As information flows back from the CC to the agents, a compromised CC will introduce false positives/negatives into the ego’s fused state. In Figs. 5b, 5d, the ego’s fused state sees many false positives compared to the baseline of Fig. 4.

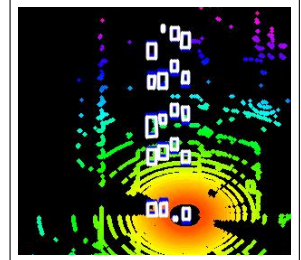
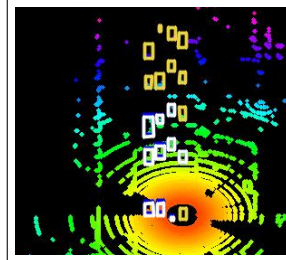
In the uncoordinated case, there is low likelihood that two adversaries will have consistent targets. The adversaries can still bring about false positives at the CC even though the attacks are uncoordinated. Without integrity, the CC is incapable of filtering out false tracks from individual agents if those false tracks are self-consistent longitudinally. However, there will be few false negatives at the CC because the same object is unlikely to be negated by multiple adversaries.



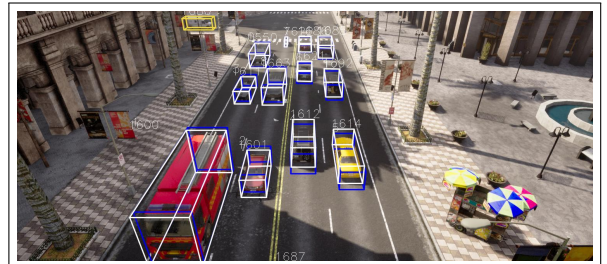
(a) Baseline: ego view with local tracks. False negatives (yellow) occur because ego suffers from occlusion.



(b) Baseline: ego view with fused tracks from CC. Occlusion mitigated; more objects detected at a longer range.

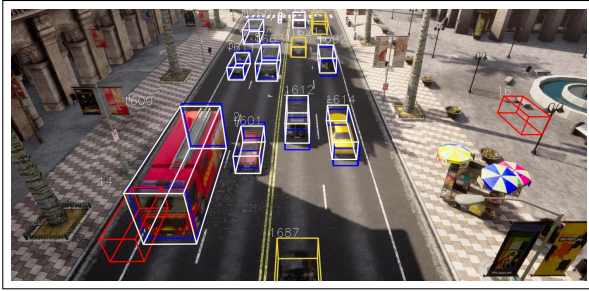


(c) Companion of (a); BEV of ego LiDAR with local information illustrates large number of false negatives in yellow. (d) Companion of (b); BEV of ego LiDAR with unconditioned CC information mitigates occlusion.

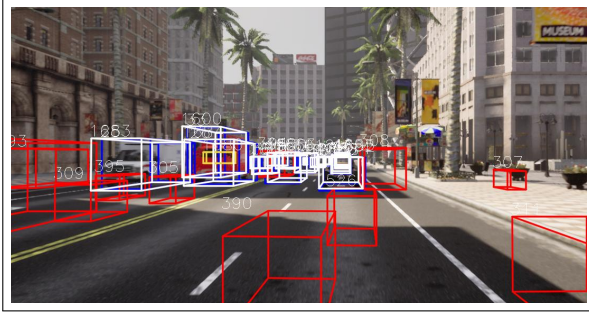


(e) Uncompromised infrastructure agent with local track states.

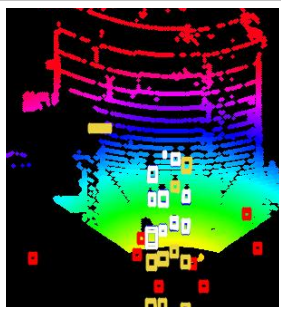
Fig. 4: Baseline: (a) Ego experiences strong occlusion in local information compared to (b) fusing multi-agent information from CC. (c, d) Bird’s-eye view (BEV) companions to (a, b) with boxes on LiDAR data. (e) An infrastructure sensor provides a collaborative vantage point on the same scene. Multiple agents can mitigate ground-vehicle occlusions.



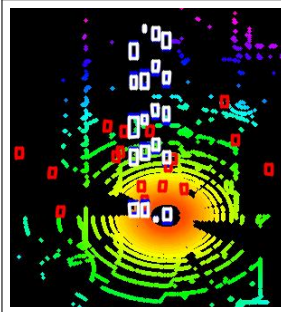
(a) *Uncoord*: agent #1 (attacked) with local tracks. False negatives (yellow) and positives (red) occur naturally *and* due to adversary.



(b) *Uncoord*: unattacked ego with fused tracks from CC. Attacked agents have compromised CC; many false positives sent to ego.



(c) Companion of (a); BEV of agent LiDAR with compromised local information.



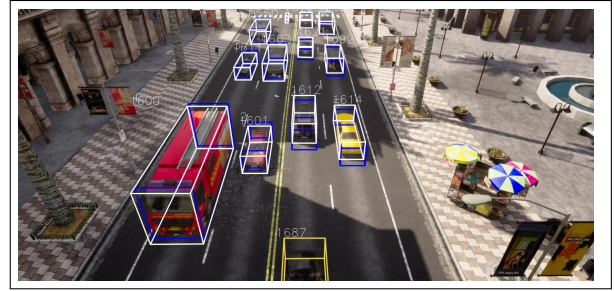
(d) Companion of (b); BEV of ego LiDAR with compromised CC information.

Fig. 5: Two of four agents are compromised in uncoordinated attack. (a) Compromised agent has attacker-induced false positives and negatives. (b) Attacks compromise CC and propagate into ego's fused state. Ego does not suffer from false negatives because other agents can correctly identify existing objects. This is due to attacks being uncoordinated. (c, d) BEV companions to (a, b) with track states marked in boxes.

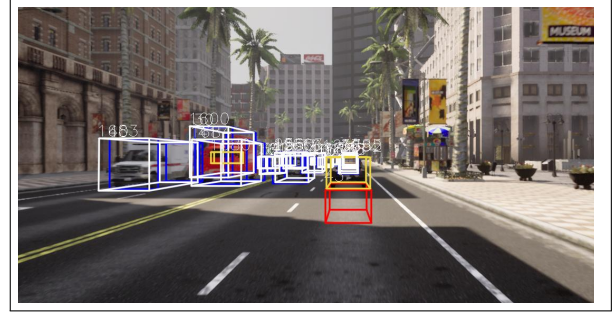
3) Coordinated Attacks

In a coordinated attack, the attack coordinator selects global targets and passes consistent attack directives back to each of the adversaries. Following the threat model of Section IV, we model coordinated attacks as compromised tracks in the multi-agent communication network. Such attacks are possible given the rise in connected vehicles and the sophistication of networking attacks [28].

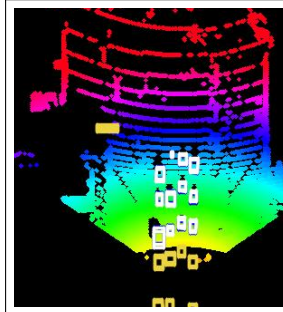
The coordinated attack parameters are identical to the uncoordinated case with the additional attack coordinator. Fig. 6 illustrates the results of the coordinated attack. False positives and negatives occur in the coordinated attack. The number of false positives is relatively lower compared to the uncoordinated case because the parameters of the lone coordi-



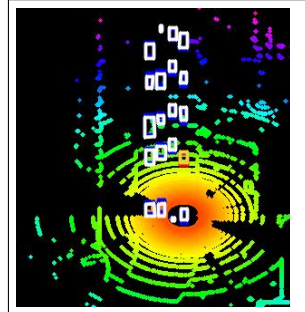
(a) *Coord*: agent #1 (attacked) with local tracks. Fewer false positives occur compared to uncoordinated due to attack parameters.



(b) *textitCoord*: ego view with fused tracks from CC. Attacked agents have compromised CC.



(c) Companion of (a); BEV of agent LiDAR with compromised local information.



(d) Companion of (b); BEV of ego LiDAR with compromised CC information.

Fig. 6: Two of four agents are compromised in coordinated attack. Outcomes similar to uncoordinated case except that fewer false positives occur. This is a result of the attack parameters set for the experiments.

nator were set identical to the parameters of *each* of the two uncoordinated adversaries. However, when integrity algorithms are introduced into the CC, we expect uncoordinated false positives to be filtered out while coordinated false positives will create persistent outcomes at the CC.

B. Monte Carlo Results

We run Monte Carlo (MC) analysis over multiple scenes and attacker parameters to illustrate MAST's effectiveness for MS/MA security analysis. We vary the following parameters and hypothesize their effects.

MC Parameters:

- **Attack type:** Coordinated vs. uncoordinated. Uncoordinated may generate more false positives due to parameters and lack of integrity at CC. Coordinated adversaries will be more successful obtaining false negatives.
- **Number of adversaries:** In the uncoordinated case

without integrity at the CC, more adversaries leads to more false positives. More adversaries enable coordinated adversaries to overcome CC integrity algorithms when present in future works.

1) Metrics

The attackers' goals are to deteriorate the CC's situational awareness by effecting changes to the agents' local fusion. To quantify the outcomes, we run baseline and attack scenarios and determine performance of each agent relative to ground truth. The set of ground truth objects is made relative to each agent and constructed as objects in the scene within a threshold distance to that agent that are visible from at least one of any of the agents (mobile or static). Given this set of truth, we compute false positive and false negative outcomes for local and fused information. We capture metrics compared to truth both for agents' local information and after the CC has redistributed aggregated tracks to each agent.

We capture the following metrics in the analysis.

MC Metrics:

- **CAFP(FN)IoB:** Compromised agent false positive/negative increment over baseline.
- **ERCCFP(FN)(TP)IoB:** Ego-relative CC false positive/negative/true positive increment over CC baseline.
- **ERCCFP(FN)(TP)IoE:** Ego-relative CC false positive/negative/true positive increment over ego's local.

2) Results

In this work, we focus on presenting the ideals of using MAST for flexible security analysis. Thus, we leave a more rigorous investigation into the MC results for future works. Many more parameters are available for MC analysis including the target selection parameters, adversary settings, ego/agent sensor fusion pipelines, and CC integrity algorithms.

Results are distilled into Table ?? . Generally, attacks induce more false positives than false negatives. This is primarily due to the inherent vulnerability of multi-agent fusion to isolated false positives. If a single agent generates a longitudinally-consistent false positive, it can propagate into a track because it is unknown whether other agents could view that object to confirm/deny it; i.e., they could simply miss the object because of occlusion. It is difficult to distinguish between "natural misses" and "adversarial misses". On the other hand, the effect on false negatives is minimal. This supports the inherent resiliency of multi-agent fusion to isolated false negatives. Collaborative agents with views of the object can compensate for object negation in a single agent.

VII. LIMITATIONS AND PLANNED IMPROVEMENTS

Perception algorithms. To emphasize the utility of the general framework, we bypassed perception algorithms online and provided detections to agents that were generated offline. Perception models are included as a part of our pipelining framework and should be included in future evaluations.

Command center integrity. We did not consider security-aware processing at the command center in the form of integrity algorithms. An investigation into the effectiveness of different schemes of centralized data integrity is a research endeavor in itself and is left to future works.

Mobile agents. We restricted the number of mobile agents based on the publicly released CARLA multi-agent dataset.

Given the released code for generating new datasets in CARLA for multi-agent research, we plan to generate richer datasets for future analysis with multiple mobile agents.

Mission-critical planning and control. The goal of the attacker was to maximally deteriorate the perspective at the command center. Commensurate with this objective, our analysis stopped at the level of the CC. Future works will fold planning and control algorithms in to this framework to assess the impact of attacks on safety and mission-critical algorithms.

VIII. CONCLUSION

We presented a multi-agent security testbed, MAST, as a scalable framework built on ROS for security analysis of multi-agent, collaborative sensor fusion. MAST leverages recently-released open-source software for multi-agent algorithms [19] and dataset generation [17]. MAST sets configuration at launch-time rather than build-time to enable diverse and rapid prototyping of AVs and manipulation of adversaries for security analysis with simple, high-level python code. We described through case studies and Monte Carlo results the effects of (un)coordinated adversaries on centralized fusion of multi-agent perception data to motivate the need for research into MS/MA integrity algorithms.

REFERENCES

- [1] "5g - v2x onward - 5gaa.org," <https://5gaa.org/5g-technology/>, [Accessed 22-12-2023].
- [2] "5gaa showcases cutting edge c-v2x technology, pioneering the future of vehicle connectivity - 5gaa," <https://5gaa.org/5gaa-showcases-cutting-edge-c-v2x-technology-pioneering-the-future-of-vehicle-connectivity/>, [Accessed 22-12-2023].
- [3] "Audi vehicles can now communicate with traffic lights in düsseldorf, germany — futurecar.com," <https://www.futurecar.com/3766/Audi-Vehicles-Can-Now-Communicate-with-Traffic-Lights-in-Düsseldorf-Germany>, [Accessed 22-12-2023].
- [4] "Lincoln mkz 2017 vehicle features," University of Michigan, Tech. Rep. [Online]. Available: https://mcity.umich.edu/wp-content/uploads/2023/03/Mcity-Vehicle-Features_2023_03_13-1.pdf
- [5] "Mcity 2.0," <https://mcity.umich.edu/our-work/mcity-test-facility/mcity-2/>, [Accessed 22-12-2023]. [Online]. Available: <https://mcity.umich.edu/our-work/mcity-test-facility/mcity-2/>
- [6] "What is V2X communication? Creating connectivity for the autonomous car era — zdnet.com," <https://www.zdnet.com/home-and-office/networking/what-is-v2x-communication-creating-connectivity-for-the-autonomous-car-era/>, [Accessed 22-12-2023].
- [7] M. Abdelfattah, K. Yuan, Z. J. Wang, and R. Ward, "Towards universal physical attacks on cascaded camera-lidar 3d object detection models," in *2021 IEEE International Conference on Image Processing (ICIP)*. IEEE, 2021, pp. 3592–3596.
- [8] J. Benko, W. Clark, C. Craig, G. Culver, P. Mahan, A. Patel, D. Voce, N. Bezzo, and G. C. Lewin, "Security and resiliency of coordinated autonomous vehicles," in *2019 Systems and Information Engineering Design Symposium (SIEDS)*. IEEE, 2019, pp. 1–6.
- [9] S. S. Blackman, "Multiple-target tracking with radar applications," *Dedham*, 1986.
- [10] S. Bono, M. Green, A. Stubblefield, A. Juels, A. D. Rubin, and M. Szydlo, "Security analysis of a cryptographically-enabled rfid device," in *USENIX*, vol. 31, 2005, pp. 1–16.
- [11] N. E. Boudette, "Tesla says autopilot makes its cars safer. crash victims say it kills." *International New York Times*, pp. NA–NA, 2021.
- [12] Y. Cao, C. Xiao, B. Cyr, Y. Zhou, W. Park, S. Rampazzi, Q. A. Chen, K. Fu, and Z. M. Mao, "Adversarial sensor attack on lidar-based perception in autonomous driving," in *Proceedings of the 2019 ACM SIGSAC conference on computer and communications security*. London, UK: ACM, 2019, pp. 2267–2281.

Run ID	Coord?	# Adv	ERCCFNIoB	ERCCFNIoE	ERCCFPIoB	ERCCFPIoE	ERCCTPIoB	ERCCTPIoE
C-1	True	1	0.00 +/- 0.00	-7.60 +/- 2.67	3.21 +/- 1.47	3.04 +/- 2.15	0.00 +/- 0.00	7.60 +/- 2.67
C-2	True	2	0.08 +/- 0.28	-7.51 +/- 2.69	5.65 +/- 2.73	5.48 +/- 3.13	-0.08 +/- 0.28	7.51 +/- 2.69
C-3	True	3	0.10 +/- 0.29	-7.50 +/- 2.68	5.74 +/- 2.63	5.56 +/- 3.03	-0.10 +/- 0.29	7.50 +/- 2.68
UC-1	False	1	0.01 +/- 0.11	-7.58 +/- 2.68	7.92 +/- 2.76	7.74 +/- 3.19	-0.01 +/- 0.11	7.58 +/- 2.68
UC-2	False	2	0.27 +/- 0.47	-7.32 +/- 2.78	15.67 +/- 5.29	15.49 +/- 5.49	-0.27 +/- 0.47	7.32 +/- 2.78
UC-3	False	3	0.33 +/- 0.50	-7.26 +/- 2.76	23.30 +/- 8.19	23.12 +/- 8.26	-0.33 +/- 0.50	7.26 +/- 2.76

(a) Ego-relative command center false negative/false positive/true positive increment over baseline/ego-local outcome. Compares CC operating picture under attack scenario to CC under unattacked baseline (IoB) and to ego’s local information (IoE).

Run ID	Coord?	# Adv	CAFNIoB_agent1	CAFNIoB_agent2	CAFNIoB_agent3	CAFPIoB_agent1	CAFPIoB_agent2	CAFPIoB_agent3
C-1	True	1	0.00 +/- 0.00	N/A	N/A	3.21 +/- 1.47	N/A	N/A
C-2	True	2	0.08 +/- 0.28	0.08 +/- 0.28	N/A	5.65 +/- 2.73	5.65 +/- 2.73	N/A
C-3	True	3	0.10 +/- 0.29	0.10 +/- 0.29	0.10 +/- 0.29	5.74 +/- 2.63	5.74 +/- 2.63	5.74 +/- 2.63
UC-1	False	1	0.01 +/- 0.11	N/A	N/A	7.92 +/- 2.76	N/A	N/A
UC-2	False	2	0.27 +/- 0.47	0.27 +/- 0.47	N/A	15.67 +/- 5.29	15.67 +/- 5.29	N/A
UC-3	False	3	0.33 +/- 0.50	0.33 +/- 0.50	0.40 +/- 1.13	23.30 +/- 8.19	23.30 +/- 8.19	23.59 +/- 7.85

(b) Compromised agent false negative/positive increment over baseline for each agent.

TABLE III: Results over 6 runs of (un)coordinated attacks with different numbers of adversaries. Metrics described in Section VI-B and illuminate agent/CC performance changes over both unattacked baseline and local-only information. Effect on false positives is much larger than false negatives. Multi-agent fusion is inherently vulnerable to isolated false positives propagating into fake objects and inherently resilient to isolated instances of false negatives when other agents can provide support.

- [13] S. Checkoway, D. McCoy, B. Kantor, D. Anderson, H. Shacham, S. Savage, K. Koscher, A. Czeskis, F. Roesner, and T. Kohno, “Comprehensive experimental analyses of automotive attack surfaces,” in *20th USENIX (USENIX Security 11)*, 2011.
- [14] G. Conte, D. Scaradozzi, D. Mannocchi, P. Raspa, L. Panebianco, and L. Screpanti, “Development and experimental tests of a ros multi-agent structure for autonomous surface vehicles,” *Journal of Intelligent & Robotic Systems*, vol. 92, pp. 705–718, 2018.
- [15] M. Contributors, “MMDetection3D: OpenMMLab next-generation platform for general 3D object detection,” <https://github.com/open-mmlab/mmdetection3d>, 2020.
- [16] R. S. Hallyburton, Y. Liu, Y. Cao, Z. M. Mao, and M. Pajic, “Security analysis of camera-lidar fusion against black-box attacks on autonomous vehicles,” in *31st USENIX (USENIX SECURITY)*. Berkeley, CA: USENIX, 2022, pp. 1–18.
- [17] R. S. Hallyburton and M. Pajic, “Datasets, models, and algorithms for multi-sensor, multi-agent autonomy using avstack,” *arXiv preprint arXiv:2312.04970*, 2023.
- [18] —, “Securing autonomous vehicles under partial-information cyber attacks on lidar data,” *arXiv preprint arXiv:2303.03470*, 2023.
- [19] R. S. Hallyburton, S. Zhang, and M. Pajic, “Avstack: An open-source, reconfigurable platform for autonomous vehicle development,” in *Proceedings of the ACM/IEEE 14th International Conference on Cyber-Physical Systems (with CPS-IoT Week 2023)*, 2023, pp. 209–220.
- [20] O. A. Ibrahim, A. M. Hussain, G. Oligeri, and R. Di Pietro, “Key is in the air: Hacking remote keyless entry systems,” in *Security and Safety Interplay of Intelligent Software Systems: ESORICS 2018 International Workshops, ISSA 2018 and CSITS 2018, Barcelona, Spain, September 6–7, 2018, Revised Selected Papers*. Springer, 2019, pp. 125–132.
- [21] R. Jonker and T. Volgenant, “Improving the hungarian assignment algorithm,” *Operations Research*, vol. 5, no. 4, pp. 171–175, 1986.
- [22] S. Julier and J. K. Uhlmann, “General decentralized data fusion with covariance intersection,” in *Handbook of multisensor data fusion*. CRC Press, 2017, pp. 339–364.
- [23] S. Kamkar, “Drive it like you hacked it: New attacks and tools to wirelessly steal cars,” *Presentation at DEFCON*, vol. 23, p. 10, 2015.
- [24] K. Koscher, A. Czeskis, F. Roesner, S. Patel, T. Kohno, S. Checkoway, D. McCoy, B. Kantor, D. Anderson, H. Shacham *et al.*, “Experimental security analysis of a modern automobile,” in *2010 IEEE symposium on security and privacy*, IEEE. New York, NY: IEEE, 2010, pp. 447–462.
- [25] M. Lee, M. Sunwoo, and K. Jo, “Collision risk assessment of occluded vehicle based on the motion predictions using the precise road map,” *Robotics and Autonomous Systems*, vol. 106, pp. 179–191, 2018.
- [26] S. Malik and W. Sun, “Analysis and simulation of cyber attacks against connected and autonomous vehicles,” in *2020 International Conference on Connected and Autonomous Driving*. IEEE, 2020, pp. 62–70.
- [27] C. Miller and C. Valasek, “Remote exploitation of an unaltered passenger vehicle,” *Black Hat USA*, vol. 2015, no. S 91, pp. 1–91, 2015.
- [28] NHTSA, “Motor vehicles increasingly vulnerable to remote exploits,” *Internet Crime Complaint Center (IC3)*, 2016. [Online]. Available: <http://www.ic3.gov/media/2016/160317.aspx>
- [29] A. Petrillo, A. Pescape, and S. Santini, “A secure adaptive control for cooperative driving of autonomous connected vehicles in the presence of heterogeneous communication delays and cyberattacks,” *IEEE transactions on cybernetics*, vol. 51, no. 3, pp. 1134–1149, 2020.
- [30] M. Quigley, K. Conley, B. Gerkey, J. Faust, T. Foote, J. Leibs, R. Wheeler, A. Y. Ng *et al.*, “Ros: an open-source robot operating system,” in *ICRA workshop on open source software*, vol. 3, no. 3.2. Kobe, Japan, 2009, p. 5.
- [31] J. Sun, Y. Cao, Q. A. Chen, and Z. M. Mao, “Towards robust {LiDAR-based} perception in autonomous driving: General black-box adversarial sensor attack and countermeasures,” in *29th USENIX (USENIX Security 20)*. Boston, MA: USENIX, 2020, pp. 877–894.
- [32] J. Tu, M. Ren, S. Manivasagam, M. Liang, B. Yang, R. Du, F. Cheng, and R. Urtasun, “Physically realizable adversarial examples for lidar object detection,” in *Proceedings of the IEEE/CVF CVPR*. New York, NY: IEEE, 2020, pp. 13716–13725.
- [33] R. Xu, H. Xiang, X. Xia, X. Han, J. Li, and J. Ma, “Opv2v: An open benchmark dataset and fusion pipeline for perception with vehicle-to-vehicle communication,” in *2022 ICRA*, 2022, pp. 2583–2589.
- [34] Q. Zhang, S. Jin, J. Sun, X. Zhang, R. Zhu, Q. A. Chen, and Z. M. Mao, “On data fabrication in collaborative vehicular perception: Attacks and countermeasures,” *arXiv preprint arXiv:2309.12955*, 2023.
- [35] B. Zou, P. Choobchian, and J. Rozenberg, “Cyber resilience of autonomous mobility systems: cyber-attacks and resilience-enhancing strategies,” *Journal of transportation security*, pp. 1–19, 2021.